Cellular/Molecular

Acid-Sensing Ion Channels Activated by Evoked Released Protons Modulate Synaptic Transmission at the Mouse Calyx of Held Synapse

Carlota González-Inchauspe, Francisco J. Urbano, Mariano N. Di Guilmi, and Osvaldo D. Uchitel

Instituto de Fisiología, Biología molecular y Neurociencias, Departamento de Fisiología, Biología Molecular y Celular "Dr. Héctor Maldonado," Facultad de Ciencias Exactas y Naturales, Universidad de Buenos Aires, Ciudad Universitaria, Ciudad Autónoma de Buenos Aires, Beunos Aires, CP 1428 EGA Argentina

Acid-sensing ion channels (ASICs) regulate synaptic activities and play important roles in neurodegenerative diseases. We found that these channels can be activated in neurons of the medial nucleus of the trapezoid body (MNTB) of the auditory system in the CNS. A drop in extracellular pH induces transient inward ASIC currents (I_{ASIC}s) in postsynaptic MNTB neurons from wild-type mice. The inhibition of I_{ASIC}s by psalmotoxin-1 (PcTx1) and the absence of these currents in knock-out mice for ASIC-1a subunit (ASIC1a $^{-/-}$) suggest that homomeric ASIC-1as are mediating these currents in MNTB neurons. Furthermore, we detect ASIC1a-dependent currents during synaptic transmission, suggesting an acidification of the synaptic cleft due to the corelease of neurotransmitter and H^+ from synaptic vesicles. These currents are capable of eliciting action potentials in the absence of glutamatergic currents. A significant characteristic of these homomeric ASIC-1as is their permeability to Ca^{2+}. Activation of ASIC-1a in MNTB neurons by exogenous H^+ induces an increase in intracellular Ca^{2+}. Furthermore, the activation of postsynaptic ASIC-1as during high-frequency stimulation (HFS) of the presynaptic nerve terminal leads to a PcTx1-sensitive increase in intracellular Ca^{2+} in MNTB neurons, which is independent of glutamate receptors and is absent in neurons from ASIC1a $^{-/-}$ mice. During HFS, the lack of functional ASICs in synaptic transmission results in an enhanced short-term depression of glutamatergic EPSCs. These results strongly support the hypothesis of protons as neurotransmitters and demonstrate that presynaptic released protons modulate synaptic transmission by activating ASIC-1as at the calyx of Held–MNTB synapse.

Key words: ASIC-1a; calyx of Held; glutamatergic EPSCs; protons; short-term depression; synaptic plasticity

Significance Statement

The manuscript demonstrates that postsynaptic neurons of the medial nucleus of the trapezoid body at the mouse calyx of Held synapse express functional homomeric Acid-sensing ion channel-1a (ASIC-1as) that can be activated by protons (coreleased with neurotransmitter from acidified synaptic vesicles). These ASIC-1as contribute to the generation of postsynaptic currents and, more relevant, to calcium influx, which could be involved in the modulation of presynaptic transmitter release. Inhibition or deletion of ASIC-1a leads to enhanced short-term depression, demonstrating that they are concerned with short-term plasticity of the synapse. ASICs represent a widespread communication system with unique properties. We expect that our experiments will have an impact in the neurobiology field and will spread in areas related to neuronal plasticity.

Introduction

Extracellular proton concentration in brain fluctuates in both physiological and disease conditions (Chesler, 2003). Increase in proton concentration or reduction in pH activate acid-sensing ion channels (ASICs; Waldmann et al., 1997a,b; Krishtal, 2003; Wemmie et al., 2006), which are part of the larger amiloride-

Received Aug. 12, 2016; revised Jan. 10, 2017; accepted Jan. 13, 2017.

Author contributions: C.G.-I., F.J.U., M.N.D.G., and O.D.U. designed research; C.G.-I. performed research; C.G.-I. and M.N.D.G. analyzed data; C.G.-I. wrote the paper.

We thank Professor John A. Wemmie from the Department of Psychiatry of The University of Iowa (Iowa City, IA), who generously provided the genetically modified ASIC1a $^{-/-}$ mice. We also thank María Eugenia Martin for her invaluable technical assistance.

This work was supported by Grants PICT 2013–2202 and PICT-2011–2667 from Agencia Nacional de Promoción Científica y Tecnológica (ANPCYT) and Grant 01/Q666 (20020130100666BA; Universidad de Buenos Aires Ciencia y Tecnología [UBACYT]) from University of Buenos Aires (to O.D.U.) and by grants from FONCYT-ANPCYT; BID 1728 OC.AR. PICT-2012–1769 and UBACYT 2014–2017 #20120130101305BA (to F.J.U.).

The authors declare no competing financial interests.

Correspondence should be addressed to Dr. Osvaldo D. Uchitel, Instituto de Fisiología, Biología molecular y Neurociencias (IFIBYNE) UBA-CONICET, Facultad de Ciencias Exactas y Naturales, Edificio IFIBYNE Ciudad Universitaria, Ciudad Autónoma de Buenos Aires, CP 1428 EGA Argentina. E-mail: ouchitel@gmail.com.

DOI:10.1523/JNEUROSCI.2566-16.2017

 0270-6474/17/372589-11$15.00/0

sensitive degenerin/epithelial Na^+ channel family (Kellenberger and Schild, 2015). ASICs play an important function in physiologic processes and signal transduction associated with local and global extracellular pH variations during normal and pathological neuronal activity. ASICs are engaged in synaptic transmission contributing to plasticity, learning, memory, and fear responses (Wemmie et al., 2002, 2006; Chu and Xiong, 2012; Huang et al., 2015). They have also been implicated in pathological conditions, including ischemic stroke (Chu and Xiong, 2012; Xiong et al., 2004; Yermolaieva et al., 2004), epileptic seizure (Ziemann et al., 2008), multiple sclerosis, and autoimmune encephalomyelitis (Friese et al., 2007).

Six different ASIC subunits, encoded by four genes, have been cloned (Kellenberger and Schild, 2015), forming homomultimeric and heteromultimeric channel complexes that vary in their expression within organs and are activated at different pH values (Krishtal, 2003; Lingueglia et al., 1997; Wemmie et al., 2003; Gründer and Pusch, 2015). ASIC-1a, ASIC-2a, and ASIC-2b are expressed in brain neurons with particularly high abundance in the cerebral cortex, hippocampus, basal ganglia, amygdala, olfactory bulb, and cerebellum (Krishtal, 2003; Chen et al., 1998; Waldmann and Lazdunski, 1998; Price et al., 2014). The subunit ASIC-1a forms heteromeric channels with ASIC-2a, and also Ca^{2+}-permeable homomeric channels (Xiong et al., 2004; Yermolaieva et al., 2004; Lingueglia et al., 1997; Waldmann et al., 1997a,b; Wu et al., 2004). ASIC-1a is enriched in synaptosomal fractions, which are expressed in dendritic spines (Hruska-Hageman et al., 2002; Wemmie et al., 2002), where channels interacts with the postsynaptic scaffolding proteins like PSD-95 and PICK1 (protein interacting with C kinase 1) and also with NMDA receptors and voltage-gated Ca^{2+} channels (Zha, 2013).

ASICs contribute to modulate synaptic transmission (Huang et al., 2015). ASIC-1a disruption increased miniature EPSC frequencies and reduced paired-pulse ratios in microisland cultures of hippocampal neurons (Cho and Askwith, 2008), impaired hippocampal long-term potentiation (Wemmie et al., 2002), and potentiated neuromuscular transmission (Urbano et al., 2014), suggesting that ASIC activation affects presynaptic release probability.

It is known that synaptic vesicles are acidic, and it is postulated that acidification of the synaptic cleft during neurotransmission might activate ASICs (Palmer et al., 2003; Hnasko and Edwards, 2012). Two studies have shown that ASICs contribute to EPSCs in both the lateral amygdala (Du et al., 2014) and nucleus accumbens core (Kreple et al., 2014), strongly supporting the concept that protons coreleased with neurotransmitters might activate ASICs.

In the present work, we sought to clarify the functional significance of proton–ASIC signaling and the role of ASIC-1a during high-frequency stimulation (HFS) of synaptic transmission at the calyx of Held–medial nucleus of the trapezoid body (MNTB) synapse by examining the effects of ASIC-1a on electrical and Ca^{2+} postsynaptic signals and on the modulation of presynaptic quantal release of neurotransmitter.

Inward ASIC currents (I_{ASIC}s) sensitive to amiloride and to the specific ASIC-1a blocker psalmotoxin were elicited in the MNTB postsynaptic neurons but not in the presynaptic nerve terminal from wild-type (WT) mice. In contrast, I_{ASIC}s were absent in the ASIC1a$^{-/-}$ mouse. ASIC-1a currents evoked by exogenous H^+ induced an increase in intracellular calcium ($Ca^{2+}{}_i$) in postsynaptic MNTB neurons. In addition, under physiological pH and pharmacological blockade of glutamate, GABA and glycine postsynaptic receptors, presynaptic stimulation-generated small I_{ASIC}s, and HFS induced an increase in $Ca^{2+}{}_i$, which can be attributed to the activation of postsynaptic ASIC-1as due to acidification of the synaptic clef. Pharmacological blockage or ablation of ASIC-1as enhanced short-term depression (STD) of glutamatergic EPSCs. These results demonstrate that presynaptic released protons activate postsynaptic ASIC-1as and modulate synaptic transmission at the calyx of Held–MNTB synapse. To our knowledge, this is the first report of an ASIC-dependent postsynaptic Ca^{2+} signal triggered by evoked presynaptic released protons in the CNS, suggesting that protons as cotransmitters are relevant for information processing.

Materials and Methods

Animal model and preparation of brainstem slices

ASIC1a$^{-/-}$ mice (generated using mice of the C57BL/6 genetic background) were provided by the laboratory of Dr. John A. Wemmie (University of Iowa, Iowa City, IA) and were kept in the animal facility of the Faculty of Exact and Natural Sciences (University of Buenos Aires, Buenos Aires, Argentina). All experiments involving mice were performed according to national guidelines and were approved by local ethical committees.

Mice of either sex were killed by decapitation on postnatal day 13 (P13) to P18, and the brain was removed and placed into ice-cold low-sodium artificial CSF (aCSF). The brainstem was mounted in the Peltier chamber of an Integraslice 7550PSDS vibrating microslicer (Campden Instruments). Transverse slices of 300 μm thickness were cut in low sodium aCSF (NaCl replaced by 250 mM sucrose, 2.9 mM $MgCl_2$, and 0.1 mM $CaCl_2$) and then transferred to an incubation chamber containing normal bicarbonate aCSF with low calcium (0.1 mM $CaCl_2$ and 2.9 mM $MgCl_2$) at 37°C for 1 h. Recordings were obtained in normal bicarbonate aCSF containing the following (in mM): NaCl 125, KCl 2.5, $NaHCO_3$ 26, NaH_2PO_4 1.25, glucose 10, ascorbic acid 0.5, myoinositol 3, sodium pyruvate 2, $MgCl_2$ 1, and $CaCl_2$ 2. The pH was 7.3 when gassed with 95% O_2-5% CO_2.

Electrophysiology recordings

H^+-gated, ASIC-mediated currents (i.e., I_{ASIC}s) and glutamatergic EPSCs on MNTB neurons were measured using whole-cell voltage clamp. Neurons were visualized using Nomarski optics on a BX50WI (Olympus) microscope, with a 40×/0.90 numerical aperture water-immersion objective lens (LUMPlane FI, Olympus).

To measure I_{ASIC}s, slices were transferred to a recording chamber perfused with an extracellular HEPES/MES-based solution at pH 7.3, containing the following (in mM): NaCl 128, KCl 2.5, $CaCl_2$ 2, $MgCl_2$ 1, glucose 15, sucrose 15, HEPES 5, MES 5, ascorbic acid 0.5, myoinositol 3, and sodium pyruvate 2. A HEPES buffering range of 6.8–8.2 allowed us to control recording solutions with a pH of ~7.3 while the MES buffering range of 5.5–6.7 allowed us to fix pH 5.5 and 6.0 used during local pressure applications.

For recording EPSCs at the calyx of Held synapse, normal bicarbonate-based aCSF at pH 7.3 was used, unless in those experiments where perfusing with HEPES/MES-based aCSF of different pH buffer capacity is indicated (low vs high physiological buffering at pH 7.3: 1 and 10 mM HEPES, respectively).

Patch pipettes were pulled from borosilicate glass (Harvard Apparatus, GC150F-15, UK). Electrodes had resistances of 2.9–3.2 MΩ when filled with internal solution of the following composition (mM): CsCl 110, HEPES 40, TEA-Cl 10, Na_2phosphocreatine 12, EGTA 0.5, MgATP 2, LiGTP 0.5, and $MgCl_2$ 1. PH was adjusted to 7.3 with CsOH. To block Na^+ currents and avoid postsynaptic action potentials (APs), 10 mM QX-314 was added to the pipette solution. In whole-cell configuration under current-clamp mode, patch solutions contained the following (mM): K-gluconate 110, KCl 30, HEPES 10, Na-phosphocreatine 10, EGTA 0.2, MgATP 2, LiGTP 0.5, and $MgCl_2$ 1.

Patch-clamp recordings were obtained using a Multiclamp 700B amplifier (Axon CNS, Molecular Devices), Digidata 1440A (Axon CNS, Molecular Devices), and pClamp 9.0 software. Data were sampled at

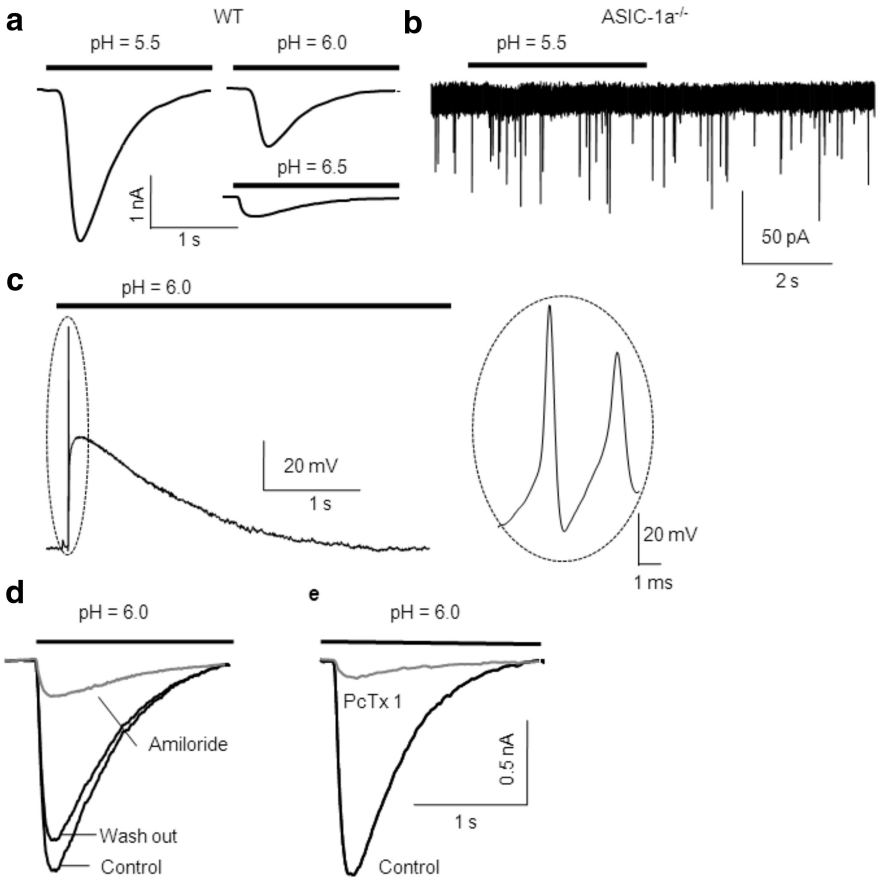

Figure 1. ASIC-1as are activated by a decrease of extracellular pH in MNTB neuron. ***a***, H^+-gated I_{ASIC}s from MNTB neurons in WT mice during transient acidification (4 s) of the extracellular media from pH 7.3 to 5.5 (mean peak amplitude, 2.5 ± 0.5 nA; n = 25), pH 6.0 (mean peak amplitude, 0.94 ± 0.22 nA; n = 20), or pH 6.5 (mean peak amplitude, 0.32 ± 0.04 nA; n = 6). MNTB neurons were whole-cell patch clamped at a holding potential of −70 mV. ***b***, Acidification of the extracellular media induced no current in ASIC1a $^{-/-}$ mice. Please note the different magnitude in the current calibration bar. ***c***, Activation of ASICs by a drop in pH from 7.3 to 6.0 induced membrane depolarization and triggered action potentials (shown in an expanded timescale in the inset at the right) in MNTB neurons from WT mice. ***d***, In the presence of amiloride (150 μM), a nonspecific ASIC blocker, the amplitudes of I_{ASIC}s triggered by dropping the pH from 7.4 to 6.0 were reduced in 82 ± 4% in WT mice (n = 12). The effect was reversible after washout. ***e***, Effect of PcTx1 (10 nM), a specific inhibitor of ASIC-1a homomers, on ASIC currents. The mean inhibition of I_{ASIC} peak value (n = 7) was 90 ± 3%.

50 kHz and filtered at 6 kHz (low-pass Bessel). Whole-cell membrane capacitances (15–25 pF) and series resistances (6–12 MΩ) were registered from the amplifier after compensation of the transient generated by a 10 ms voltage step and compensated by 50–60%.

EPSCs were evoked by stimulating the globular bushy cell axons in the trapezoid body using a bipolar platinum electrode placed in the midline and applying square pulses (0.1 ms and 4–10 V) through an isolated constant-current stimulator (model DS3, Digitimer).

Proton (H^+)-gated currents were evoked by local application of a puff with a duration of 3–4 s of a 10 mM MES-based aCSF solution at pH 5.5, 6.0, or 6.5 using a micropipette (1.5–2 MΩ resistance) connected to a Picrospritzer (Intracel). In a few experiments, H^+ iontophoresis was used to evoke ASIC currents. A micropipette (>20 MΩ resistance) filled with 0.1 M HCl was connected to a Master-8 (A.M.P.I.) general purpose stimulator through a monopolar wire. Positive current pulses (2 nA, 3 s duration) were used to release H^+ from the pipette placed near the MNTB neurons.

Data analysis was performed using Clampfit 10.0 (Molecular Devices), and SigmaPlot 10.0, SigmaStat 3.5, and Excel 2003 (Microsoft). Data are expressed the average and were plotted as the mean ± SEM. Statistical significance was determined using paired or unpaired Student's t test or one-way repeated-measures ANOVA plus Student–Newman–Keuls *post hoc* test.

Psalmotoxin 1 (PcTx1) was purchased from Alomone Labs and lactic acid from Anedra.

Fluorescence measurements

For Ca^2 image acquisition, we used a BX51WI upright microscope with a 60× objective lens (Olympus) and an electron multiplying CCD camera (Andor iXon, Oxford Instruments), together with cell^M System Coordinator/ cell^R real time controller software. MNTB neurons were loaded with the high-affinity Ca^{2+} indicator Fluo 8 in salt form, added to a final concentration of 100 μM to the CsCl-based patch solution with no EGTA. The excitation and emission wavelengths were 488 and 515 nm, respectively. Off-line image processing was performed using ImageJ. To analyze time-dependent fluorescence changes, we normalized mean fluorescence values as follows. First, the average Ca^{2+} fluorescence signal in a region of the cells was "background corrected" by subtraction of the average measured signal from an extracellular region. The background-corrected fluorescence measured in each image frame during the protocol was then subtracted from the mean fluorescence measured in the first images acquired under initial control conditions (F_0, line base before activating ASIC-1a) and finally normalized to F_0. This procedure subtracts autofluorescence and the present data as the Fluo 8 fluorescence (ΔF) normalized to basal fluorescence (F_0; $\Delta F/F_0$).

Results

Acid-sensing ion channels are proton receptors and generate inward currents in MNTB neurons

Local acidification induced I_{ASIC}s in MNTB neurons from WT mice (holding membrane potential, −70 mV). On average, a pH drop from 7.3 to 5.5, 6.0, and 6.5 elicited I_{ASIC}s with peak amplitudes of 2.4 ± 0.2 nA (n = 25), 1.1 ± 0.2 nA (n = 20), and 0.32 ± 0.04 nA (n = 6) respectively, as shown in Figure 1*a*. As a control, application of a puff of pH 7.3 solution did not induce any significant current (data not shown; n = 4 MNTB neurons). Furthermore, extracellular application of a pH 5.5 or 6.0 solution did not evoke any current in neurons from ASIC1a $^{-/-}$ mice (n = 3 MNTB neurons; Fig. 1*b*).

Under the same conditions as for postsynaptic neurons, we did not detect ASIC-mediated presynaptic currents when presynaptic terminals were patch clamped at −70 mV while applying an exogenous puff of either pH 5.5 or 6.0 extracellular solution (n = 12).

ASIC activation depolarizes membrane potential, reaching action potential threshold in MNTB neurons

Current-clamp experiments were conducted to record membrane potential in MNTB neurons during acidification. A drop in extracellular pH from 7.3 to 6.0 induced significant membrane depolarization from a resting membrane potential of −65 to −25 mV (Fig. 1*c*; n = 3 MNTB neurons), together with one or more action potentials (Fig. 1*c*, right). These results indicate that ASICs activation can contribute to the integration of excitatory inputs at MNTB neurons.

Pharmacological profiles of I_{ASIC}s in MNTB neurons

Amiloride, a diuretic agent that inhibits Na^+/H^+, Na^+/Ca^{2+} antiporters, and ENaC, is a nonselective inhibitor for ASICs, which acts blocking their pore. At the MNTB neurons, amiloride (150 μM) reduced the amplitudes of I_{ASIC}s, in a reversible manner, to 82 ± 4% in WT mice ($n = 12$) when pH was dropped from 7.3 to 6.0 (Fig. 1*d*). The spider peptide toxin PcTx1 has been shown to specifically block homomeric ASIC-1as (Escoubas et al., 2000; Chen et al., 2006). In our experiments, I_{ASIC}s were almost abolished by PcTx1 (10 nM) in MNTB neurons from WT mice (Fig. 1*e*; $n = 7$). These data, together with the absence of acid-evoked currents in ASIC1a$^{-/-}$ mice suggest that ASICs in MNTB neurons are ASIC-1a homomers.

Desensitization and recovery of ASIC-1a-mediated currents

It has been reported that during maintained application (3–4 s) of a pH 6.0 solution, ASIC-1a-mediated currents inactivate (Li et al., 2012). Inactivation was characterized by measuring the half-width (HW; at 50% amplitude) and decaying time (DT; at 90–10% amplitude) of the currents evoked by application of a 4-s-long puff of pH 6.0 solution. In WT mice, the mean HW of I_{ASIC}s was 678 ± 50 ms, and the mean DT was 1.21 ± 0.08 s ($n = 20$). Repetitive local acidifications desensitized ASIC-1a currents. Successive acidic pulses of pH 6.0 solutions with a duration of 3 s were applied at 10 s intervals, eliciting transient ASIC-1a currents with progressively lower peak amplitudes (Fig. 2*a*). The time course of the successive I_{ASIC} amplitudes (normalized to the peak amplitude of the first I_{ASIC}) was well fitted to a single exponential decay function (Fig. 2*b*; $n = 6$).

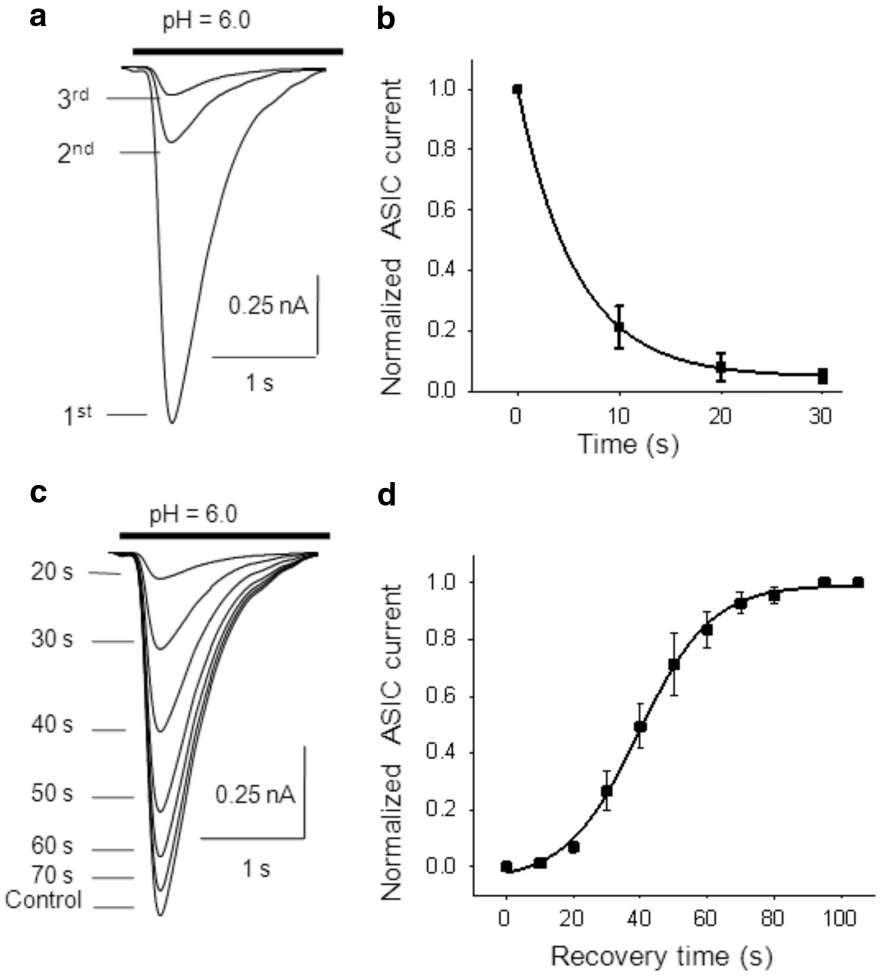

Figure 2. Desensitization of ASIC-1as. ***a***, Representative ASIC currents activated by successive 3-s-long acidic puffs of a pH 6.0 solution at 10 s intervals, showing ASIC desensitization (transient ASIC-1a currents with progressively lower peak amplitudes). ***b***, ASIC current amplitudes as a function of time during repetitive activation of ASICs, normalized to the first evoked I_{ASIC}. Desensitization time constant (τ_D) calculated by fitting to a single-exponential equation was $\tau_D = 5.7 \pm 0.8$ s ($n = 6$). ***c***, After the desensitization of ASIC currents by three successive 3-s-long acidic puffs of pH 6.0 (10 s interval), recovery was determined by returning the pH of the extracellular solution to 7.4 for different time intervals (from 20 to 120 s) and then applying a test 3-s-long puff at pH 6.0. Recovery was quantified as the ratio between the peak current amplitude in response to the test pH 6.0 puff and the first peak current amplitude before desensitization (control). ***d***, Time course of recovery of ASIC current amplitudes after desensitization, fitted by a sigmoid function: $I = 1/[1 + \exp((t - \tau_R)/k)]$. The time for half-recovery (τ_R) was 39.5 ± 0.7 s, and the slope k was 10.8 ± 0.7 s ($n = 6$).

To study the recovery of I_{ASIC} from desensitization, we used three consecutive 3 s duration acidic pulses to pH 6.0 at 10 s intervals, followed by a 3 s duration acidic test pulse separated by different time intervals (representative traces in Fig. 2*c*). Recovery was calculated as the ratio between the I_{ASIC} amplitudes of the test pulse and the first pulse before desensitization. Recovery as a function of time was best fitted by a sigmoid function with a time for half recovery of 39.5 ± 0.7 s (Fig. 2*d*; $n = 6$).

Current–voltage relationship of ASIC-1a currents in MNTB neurons

To investigated the current–voltage (*I–V*) relationship of ASIC-1a currents, MNTB neurons were successively patch clamped at different membrane potentials, from −70 mV to +60 mV, every 2 min to allow full recovery of I_{ASIC} (representative traces in Fig. 3*a*). The *I–V* curve (Fig. 3*b*; $n = 6$) presents the peak amplitudes of I_{ASIC}s induced by a 3 s duration decrease in pH values from 7.3 to 6.5 at different membrane potentials. I_{ASIC}s had a reversal potential close to +30 ± 5 mV ($n = 6$), suggesting that ASIC-1as in MNTB neurons were mainly permeable to Na^+ ions, together with a small but significant permeability to Ca^{2+} (see below).

ASIC-1a activation in MNTB neurons increased intracellular Ca^{2+}

It has been reported that homomeric ASIC-1as are permeable to Ca^{2+} (Xiong et al., 2004, 2006; Yermolaieva et al., 2004). To investigate whether Ca^{2+} might enter MNTB neurons during ASIC-1a activation, we evoked I_{ASIC}s by H^+ iontophoresis (see Materials and Methods). To estimate transient changes in $[Ca^{2+}]$ produced by the opening of ASIC-1as, the high-affinity Ca^{2+} indicator Fluo 8 was loaded into MNTB neurons. Upon binding to calcium, this dye exhibits an increase in fluorescence emission intensity. Calcium-mediated fluorescence images were taken before and after H^+ ejection from the pipette with a time interval of

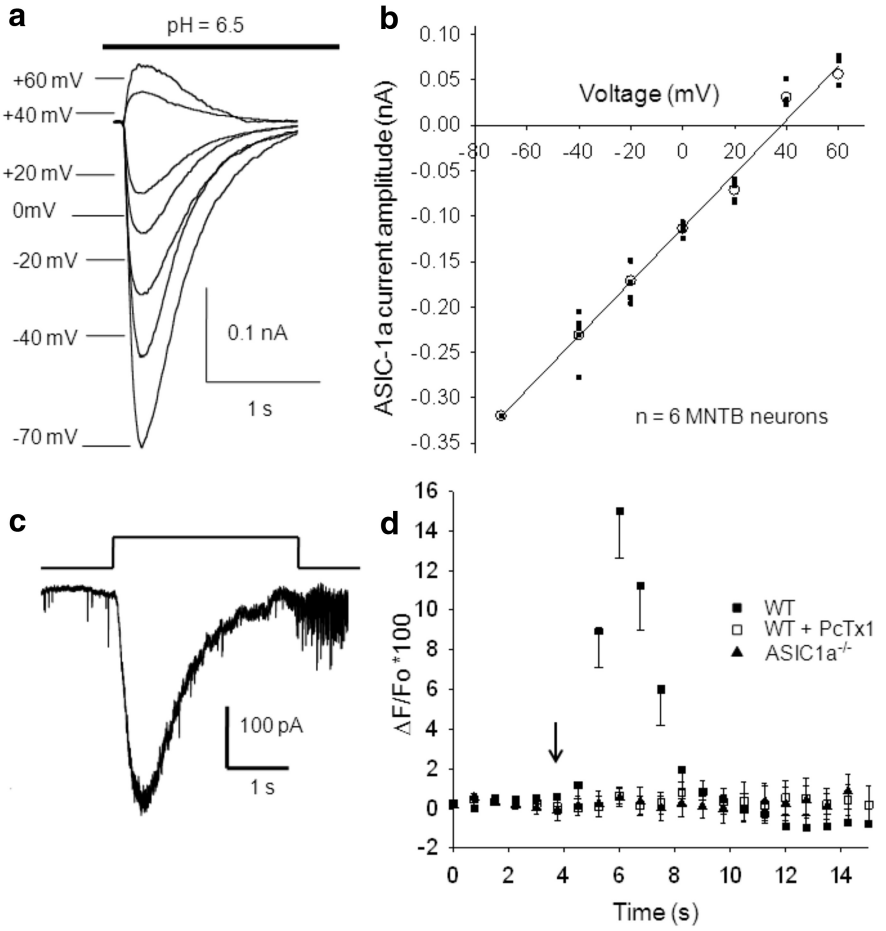

Figure 3. Voltage dependence of ASIC currents and ASIC permeability to Ca^{2+}. ***a***, Representative traces showing I_{ASIC}s activated by a 3-s-long pH drop from 7.3 to 6.5 while MNTB neurons were whole-cell patch clamped at different holding potentials. After returning to pH 7.3, cells were allowed to recover for 2 min. ***b***, Mean *I–V* plot for ASIC currents activated by a 3-s-long pH drop from 7.3 to 6.5 ($n = 6$). The detection of calcium transients evoked during the activation of ASIC-1as by H^+ injection. ***c***, Representative traces of ASIC currents evoked by H^+ iontophoresis in WT mice. The bar indicates the positive current pulse (2 nA, 3 s-duration) applied to a micropipette filled with HCl 0.1 M through a monopolar filament. ***d***, Changes in calcium-sensitive indicator $\Delta F/F_0$ as a function of time. The arrow indicates the time of iontophoretic injection of H^+. In MNTB neurons from WT mice, the Ca^{2+}-dependent fluorescence rises up to 15 ± 3% (filled squares, $n = 9$), indicating that Ca^{2+} enters into the MNTB neuron through ASIC-1as when these are activated by H^+. This increment in $[Ca^{2+}]$ is abolished when PcTx1 is applied to the bath solution (open squares; $n = 8$) and was not observed in MNTB neurons from ASIC1a $^{-/-}$ mice (filled triangles; $n = 4$).

750 ms. To generate curves of dye fluorescence intensity versus time, we used data from the background-corrected, normalized fluorescence images, as described in Materials and Methods. Figure 3*c* shows an example of I_{ASIC}s evoked by a 3-s-duration iontophoretic current. I_{ASIC}s have mean peak amplitudes of 0.48 ± 0.03 nA, mean half-widths of 0.74 ± 0.05 s, rise times of 0.31 ± 0.04 s, and decay times of 1.4 ± 0.1 s ($n = 9$). Figure 3*d* (filled squares, $n = 9$) depicts the average ratio $\Delta F/F_0$ as a function of time, showing a Ca^{2+}-dependent increase in fluorescence (maximum, 15 ± 3%; $n = 9$) after ASIC-1a channel activation in MNTB neurons from WT mice. This increment in $[Ca^{2+}]$ was inhibited by PcTx1 (Fig. 3*d*, open squares; $n = 8$ MNTB neurons from WT mice) and was not observed in MNTB neurons from ASIC1a $^{-/-}$ mice (Fig. 3*d*, filled triangles; $n = 4$ neurons).

Protons released during presynaptic stimulation contribute to postsynaptic currents

Studies in the lateral amygdala (Du et al., 2014) and nucleus accumbens core (Kreple et al., 2014), where both ASIC-1a and AISC-1a/2a are expressed, have shown a small contribution to EPSCs by ASICs activated by presynaptic stimulation. To investigate the possible activation of ASICs by protons released presynaptically, we measured evoked EPSCs in the calyx MNTB neurons while electrically stimulating the presynaptic axons (see Materials and Methods). After pharmacologically blocking AMPA, NMDA, GABA and glycine receptors with 6-cyano-7-nitroquinoxaline-2,3-dione (CNQX; 40 μM), (2R)-amino-5-phosphonovaleric acid (D-APV, 50 μM), bicuculline (20 μM), and strychnine (2 μM), respectively, we could detect amiloride and PcTx1-sensitive postsynaptic currents (Fig. 4*aI*, *aII*). These currents detected in the postsynaptic neurons occurred in the same time frame as the AMPA-mediated EPSCs. Their amplitudes (46 ± 3 pA) were remarkably smaller compared with glutamatergic EPSCs amplitudes and also compared with ASIC-1a currents evoked by exogenous H^+. They have longer half-widths and decay times compared with glutamatergic EPSCs, as shown in Figure 4*b* (Student's *t* test, $p < 0.001$; $n = 27$ MNTB neurons). Traces of these currents at different membrane potentials, as illustrated in Figure 4*c*, show that they have a reversal potential at positive voltages, as observed with prolonged extracellular acidification. These currents were absent in the ASIC1a $^{-/-}$ mice, confirming that they are mediated by ASIC-1a (Fig. 4*aIII*). Furthermore, increasing the pH buffering capacity using a 10 mM HEPES/MES-based extracellular solution (pH 7.3) in the ASIC-1a-dependent currents in MNTB neurons from WT mice was inhibited (Fig. 4*d*; $n = 6$). They were also abolished when ASIC-1as were desensitized using a 1 mM HEPES/MES-based extracellular solution at pH 6.0 (Fig. 4*e*; $n = 3$). These results support the idea that synaptic vesicle content released on the synaptic cleft upon stimulation of the calyx of Held presynaptic terminal includes glutamate and protons that activate postsynaptic ASICs.

Are the ASIC-dependent signals relevant to synaptic transmission?

To investigate the physiological relevance of ASICs, we performed current-clamp recordings to determine whether synaptic released H^+ were sufficient to trigger APs. We first recorded ASIC-1a-mediated EPSCs, visualized by blocking postsynaptic receptors with 2,3-dihydroxy-6-nitro-7-sulfonyl-benzo[*f*]quinoxaline (NBQX; 10 μM), a higher-affinity AMPA receptor antagonist, plus D-APV (50 μM), bicuculline (20 μM), and strychnine (2 μM), evoked by 100 Hz stimulation of presynaptic axons (Fig. 4*f*, top, black trace) and then switched to current-clamp mode. The resting potential of the neurons considered in the analysis varied between −60 and −65 mV, with no current injection applied. In those conditions, we observed that ASIC-1a EPSCs were able to evoke APs whose amplitudes and kinetics did not differ from those evoked by glutamatergic currents (Fig. 4*f*, bottom, black trace). PcTx1 inhibited both ASIC-1a-mediated currents and evoked APs. However, ASIC-1a-mediated

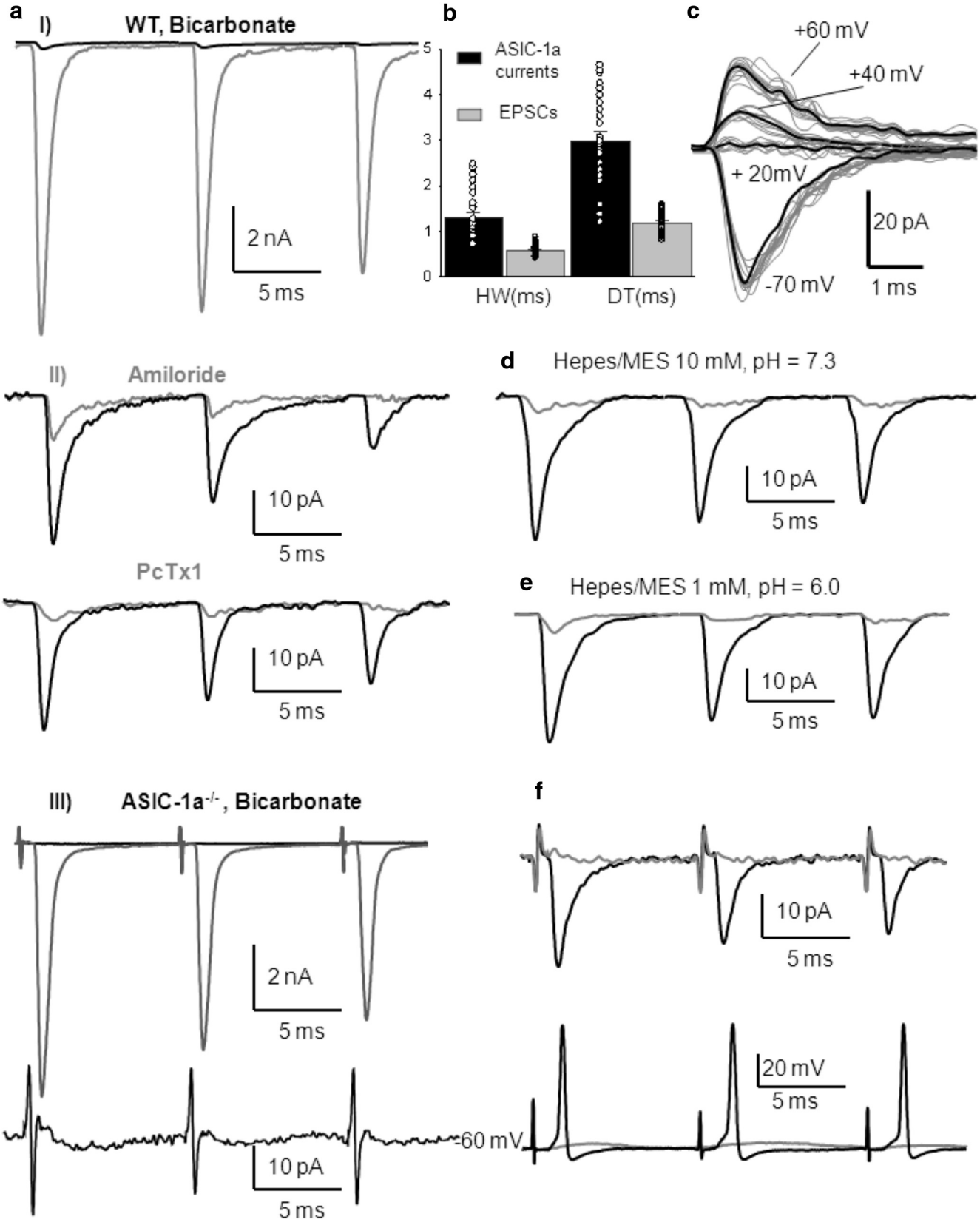

Figure 4. Blockage of glutamatergic EPSCs reveals that protons released from presynaptic vesicles elicit postsynaptic ASIC-mediated currents and action potentials in MNTB neurons from WT mice. ***al***, Representative traces of EPSCs before (gray) and after (black) blocking AMPA, NMDA, GABA, and glycine receptors with CNQX (40 μM), D-APV (50 μM), bicuculline (20 μM), and strychnine (2 μM) in an MNTB neuron from a WT mouse [postnatal day 15 (P15)]. ***all***, Higher magnification of the ASIC-1a-mediated currents insensitive to CNQX, APV, bicuculline, and strychnine (black). Mean amplitudes were 46 $\pm$ 3 pA ($n = 27$). These ASIC-1a-mediated currents were highly reduced by amiloride (top, gray trace; $n = 15$) and were inhibited by PcTx1 (bottom, gray trace; $n = 4$). ***alll***, Top, Representative traces of EPSCs before (gray) and after (black) blocking AMPA, NMDA, GABA, and glycine receptors with CNQX (40 μM), D-APV (50 μM), bicuculline (20 μM), and strychnine (2 μM) in an MNTB neuron from ASIC1a $^{-/-}$ mouse (P16). Bottom, Higher-magnification image showing the absence of any current after postsynaptic receptor (*Figure legend continues*.)

currents seem not to be very relevant in triggering postsynaptic action potential in physiological conditions since neither the fidelity of glutamatergic EPSCs nor the pattern and reliance of AP generation evoked by 100 Hz stimulation of presynaptic axons are affected in ASIC1a $^{-/-}$ mice compared with WT mice when AMPA receptors are functional. Moreover, in a series of experiments where MNTB postsynaptic action potentials in WT mice were recorded extracellularly by a pipette filled with extracellular solution and in a loose patch-clamp configuration, the input/output relation at 150 and 300 Hz stimulation (500 ms) was not altered by applying PcTx1 or increasing the buffer capacity with a 10 mM HEPES-based solution. These results indicate that in normal physiological conditions, the activation of ASIC-1as are contributing neither to AP patterns nor to the fidelity of the synaptic transmission.

During HFS, presynaptic released protons leads to an increase in intracellular Ca^{2+} in MNTB neurons through the activation of ASIC-1as

The observed ASIC-1a-mediated current contribution to the EPSC elicited by presynaptic nerve terminal stimulation makes it plausible that postsynaptic ASIC-1a channel activation in MNTB could permeate Ca^{2+} in generating a growing signal that might became detectable during the stimulation period.

To test this hypothesis, we stimulated presynaptic terminals at 150 Hz during 0.4 s and recorded glutamatergic EPSCs while simultaneously measuring the fluorescence emitted by the high-affinity Ca^{2+} indicator Fluo 8 loaded into MNTB neurons. Fluorescent images were taken every 140 ms (the first six images before stimulation as baseline) in normal bicarbonate-based aCSF containing NMDA, GABA, and glycine receptors antagonists (D-APV, 50 μM; bicuculline, 20 μM; strychnine, 2 μM). Only neurons with negligible leak current (and so stable resting potential) were considered in the analysis. During HFS, EPSCs underwent STD, as will be detailed in the next section, while an increase in fluorescence was observed in MNTB neurons from WT mice, mainly due to Ca^{2+} influx through AMPA receptors. Figure 5*a* (left, filled squares; control, $n = 9$) shows an average $\Delta F/F_0$ versus time curve, with a peak $\Delta F/F_0$ of 28 ± 5%. After AMPA/kainate glutamate receptor inhibition with CNQX (40 μM), a small increment in fluorescence remained during 150 Hz stimulation (Fig. 5*a*, left, open squares; CNQX, peak $\Delta F/F_0 = 3.8 \pm 0.9\%$). Psalmotoxin, the specific ASIC-1a blocker, inhibited this residual fluorescence increment (Fig. 5*a*, left, circles, +PcTx1), suggesting that the observed rise in intracellular Ca^{2+} was due to the activation of ASIC-1as in MNTB neurons during high-frequency synaptic activity. Applying blockers in reverse order, the maximum increase in fluorescence of 29 ± 2% recorded in control conditions during 150 Hz stimulation (Fig. 5*a*, right, filled squares; control, $n = 10$) was reduced to 24 ± 3% after inhibiting ASIC-1as with PcTx1 (Fig. 5*a*, right, circles, +PcTx1). The addition of CNQX abolished any Ca^{2+} influx, as observed by the absence of fluorescence increase (Fig. 5*a*, right, open squares, +CNQX). Therefore, inhibiting glutamate AMPA/kainate receptors reveals that these receptors contribute to ~86 ± 4% of the whole Ca^{2+} influx, while blocking ASIC-1as indicates that nearly 17 ± 3% of the full amount of Ca^{2+} influx is mediated by these channels during high-frequency synaptic activity.

To further corroborate these data, we studied the reliance of ASIC-dependent intracellular Ca^{2+} increment with the pH buffer capability. If the intracellular Ca^{2+} increase was due to the opening of ASIC-1as during acidification, then a change in the pH buffering capacity of the aCSF would affect the increase in fluorescence of the Fluo 8 Ca^{2+} indicator. In effect, using a low pH buffer capacity (HEPES 1 mM/MES) aCSF (pH 7.3), we found results similar to those obtained in normal bicarbonate-based aCSF, concerning the maximum increase in fluorescence induced during HFS in MNTB neurons from WT mice, both in control conditions (peak $\Delta F/F_0 = 28 \pm 8\%$, $n = 9$ MNTB neurons; Fig. 5*b*, filled squares, HEPES 1.0 mM/MES) and after AMPA and NMDA glutamate receptor inhibition with CNQX and D-APV (peak $\Delta F/F_0 = 3.2 \pm 0.8\%$, $n = 9$, Fig. 5*b*, open squares, HEPES 1.0 mM/MES, CNQX+APV). When slices were subsequently perfused with a high pH buffer capacity (10 mM HEPES/MES) aCSF (pH 7.3), with the addition of CNQX and D-APV, the remaining fluorescence was occluded (Fig. 5*b*, circles, HEPES 10 mM/MES, CNQX+APV).

The same experiments performed with ASIC-1a $^{-/-}$ mice using bicarbonate-based aCSF, showed an increment in intracellular Ca^{2+} during 150 Hz frequency stimulation that was not significantly different from those performed with WT mice (Fig. 5*c*, filled triangles; control, $n = 8$ MNTB neurons), with a peak $\Delta F/F_0 = 26 \pm 5\%$ ($p > 0.05$, Student's *t* test, WT vs ASIC-1a $^{-/-}$ mice). After blocking glutamate receptors with 40 μM CNQX and 50 μM D-APV, no significant changes in fluorescence were observed during or after 150 Hz stimulation (Fig. 5*c*, open triangles, CNQX plus APV; $n = 8$ MNTB neurons). These results show that a calcium-mediated postsynaptic signal is directly triggered by presynaptically evoked release of protons.

ASICs modulate synaptic plasticity at the calyx of Held–MNTB synapse

Is transmitter release affected by ASIC-1as? The activation of postsynaptic ASIC-1as as a result of HFS of the presynpatic calyx suggests that an acidification of the synaptic cleft is transiently induced and may modulate transmitter release. To investigate this subject, we recorded AP-evoked EPSCs from MNTB neurons in whole-cell voltage clamp at a resting potential of −70 mV in normal bicarbonate-based aCSF. There were no significant differences in peak amplitudes or time constants of EPSCs between WT and ASIC1a $^{-/-}$ mice [WT mice: peak amplitude = 8.6 ± 0.4 nA, $n = 42$; ASIC1a $^{-/-}$ mice: peak amplitude, 8.9 ± 0.5 nA, $n = 21$ (Student's *t* test, $p = 0.19$); WT mice: decay time constant = 1.1 ± 0.2 ms; ASIC1a $^{-/-}$ mice: decay time constant = 1.2 ± 0.3 ms (Student's *t* test, $p = 0.33$); WT mice: half-width = 0.61 ± 0.04; ASIC1a $^{-/-}$ mice: half-width = 0.69 ± 0.05 ms (Student's *t* test, $p = 0.28$); WT mice: rise time = 0.19 ± 0.01; ASIC1a $^{-/-}$ mice: rise time = 0.21 ± 0.01 ms (Student's *t* test, $p = 0.44$)].

To study synaptic plasticity, we evoked synaptic response at repetitive HFS (300 Hz, 20 stimuli). HFS at the calyx of Held–MNTB synapse caused STD; EPSC amplitudes decreased during

←

(*Figure legend continued.*) inhibition. ***b***, Mean half-width and decay time of amiloride and PcTx1-sensitive ASIC-1a-mediated currents compared with glutamatergic EPSCs (HW: 1.31 ± 0.1 ms vs 0.59 ± 0.03 ms; DT: 3.0 ± 0.2 ms vs 1.18 ± 0.05 ms; $n = 27$; Student's *t* test, $p < 0.001$). ***c***, Sample traces of ASIC-1a currents at different membrane potentials in WT mouse (P14). ***d***, Increasing pH buffering using a 10 mM HEPES-based extracellular solution, pH 7.3, the ASIC-1a-mediated currents in MNTB neurons from WT mice were highly reduced (traces from a P15 mouse). ***e***, ASIC-1a-mediated currents were highly diminished when the HEPES-based extracellular solution was maintained at pH 6.0 due to the desensitization of ASICs (traces from a P17 mouse). ***f***, ASIC-1a-mediated currents (top, black trace) evoked by 100 Hz stimulation of presynaptic axons after the blockage of postsynaptic receptors with NBQX (a higher-affinity AMPA receptor antagonist, 10 μM) plus D-APV (50 μM), bicuculline (20 μM), and strychnine (2 μM) in a P15 WT mouse. Mean amplitudes were 38 ± 8 pA (HW, 1.1 ± 0.2 ms; DT, 2.7 ± 0.3 ms; $n = 7$). These currents were able to evoke APs (measured in current-clamp configuration at the resting potential of the MNTB neurons) whose amplitudes and kinetics did not differ from those evoked by glutamatergic currents (bottom, black trace; current-clamp recording). PcTx1 inhibited both ASIC-1a-mediated currents and evoked APs (gray traces).

the train of stimuli until they reached a steady state (Fig. 6*a*). Plots of mean EPSC amplitudes as a function of time during 300 Hz stimulation, with the corresponding parameters of the exponential decay fitting are shown in Figure 6*b*. EPSCs exhibited stronger STD and a faster decay time course (τ) in ASIC1a $^{-/-}$ mice than in WT mice ($p < 0.05$, one-way ANOVA).

PcTx1 has no effect on single AP-evoked EPSCs in WT mice, but it does have an effect on STD, replicating the results observed in ASIC-1a $^{-/-}$ mice. Figure 6*c* shows the time course dependence of EPSC amplitudes during 300 Hz stimulation before and after the application of PcTx1 (10 nM), fitted by the corresponding single exponential decay function ($n = 9$). The inset represents the decay time constants (τ) in the absence and presence of PcTx1 in the aCSF for each neuron, together with the mean τ values. There is a significant increase in STD when ASIC-1as are blocked by PcTx1 ($p = 4 \times 10^{-5}$; paired Student's *t* test).

To further corroborate that ASIC-1as are activating during HFS and modulating STD, the same experiments were performed in two solutions with different pH buffer capacities. STD measured in slices from WT mice in a low H^+ buffer capacity (1 mM HEPES/MES) aCSF was attenuated with respect to that measured in a high H^+ buffer capacity (10 mM HEPES/MES) aCSF, as shown in Figure 6*d*. The inset shows the decay time constants (τ) of STD in $n = 8$ MNTB neurons, measured sequentially in the 1 and 10 mM HEPES-based aCSF, jointly with the corresponding mean τ values. There is a significant increase in STD when acidification is inhibited by the high H^+ buffer capacity of the 10 mM HEPES solution ($p < 0.001$, paired Student's *t* test).

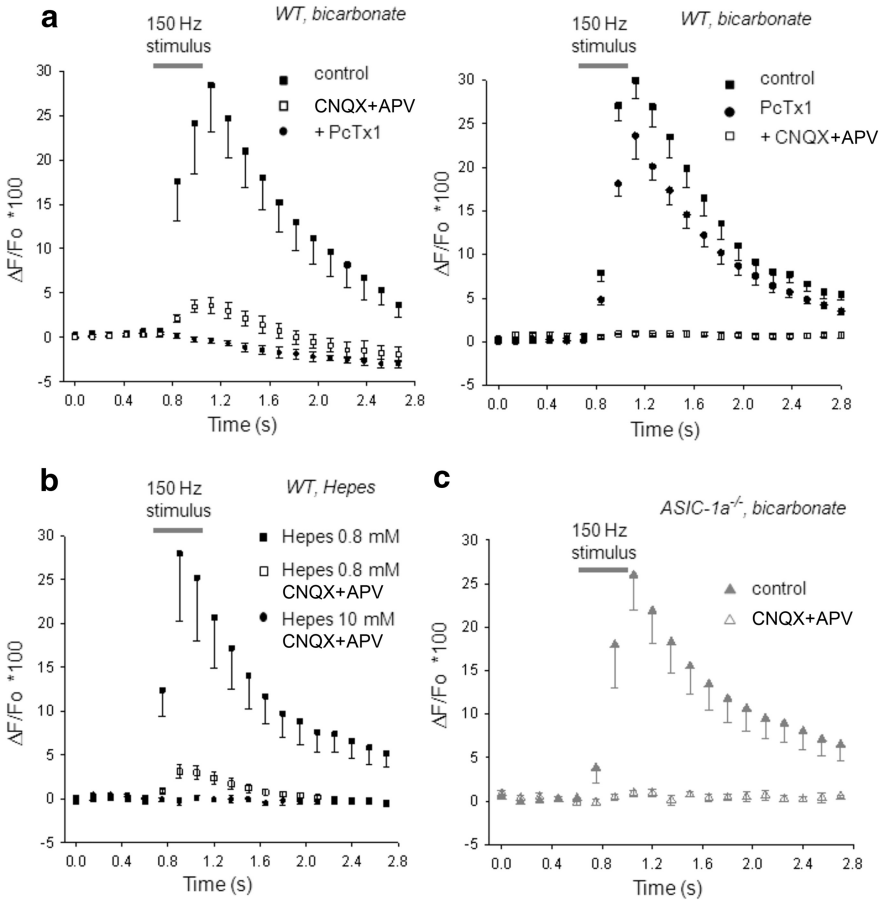

Figure 5. ASIC-1a-dependent increase of intracellular Ca^{2+} in MNTB neurons during HFS. ***a***, Time course of the Fluo 8 fluorescence emission ratio ($\Delta F/F_0$) in postsynaptic MNTB neurons from WT mice ($n = 9$) during presynaptic HFS (150 Hz, 0.4 s; indicated by gray bar) in normal bicarbonate-based aCSF. Images were taken every 140 ms (first six images before stimulation served as the baseline). Left, During HFS, a maximum increase in intracellular Ca^{2+} of 28 ± 5% ($n = 9$) is observed (filled squares; control). After AMPA/kainite glutamate receptor inhibition with 40 μM CNQX (open squares, CNQX), a small component of the fluorescence increment (peak, 3.8 ± 0.9%; $n = 9$) remained during 150 Hz stimulation. PcTx1 inhibited this residual fluorescence (circles, + PcTx1; $p < 0.05$, one-way repeated-measure ANOVA). Right, Applying drugs in reverse order, PcTx1 reduced the maximum increase in intracellular Ca^{2+} of 29 ± 2% in control conditions ($n = 10$; filled squares, control) to 24 ± 3% (circles, PcTx1), while the addition of CNQX abolished any increase in fluorescence during 150 Hz stimulation (open squares, CNQX). ***b***, Changing the pH buffer capacity of the aCSF alters ASIC-1a-dependent Ca^{2+} entry in MNTB neurons from WT mice. Plot of $\Delta F/F_0$ versus time during HFS in a low-pH buffer capacity aCSF before (filled squares, HEPES 1 mM; peak increase, 28 ± 8%; $n = 9$) and after the inhibition of glutamate AMPA and NMDA receptors (open squares, HEPES 1 mM plus CNQX + APV; peak increment, 3.2 ± 0.8%, $n = 9$). This remaining fluorescence component that may be attributed to Ca^{2+} influx through ASIC-1as was eliminated when a high-pH buffer capacity aCSF inhibits acidification (circles, HEPES 10 mM; $n = 9$; $p < 0.05$, one-way repeated-measures ANOVA). ***c***, Time course of $\Delta F/F_0$ in postsynaptic MNTB neurons from ASIC1a $^{-/-}$ mice during HFS (150 Hz, 0.4 s) in normal bicarbonate-based aCSF (filled triangles, control; $n = 8$). The maximum increase in [Ca^{2+}] through AMPA receptors (26 ± 5%) is not statistically different from that observed in WT mice ($p > 0.05$, Student's *t* test, WT vs ASIC-1a $^{-/-}$). After glutamate AMPA and NMDA receptor inhibition, the increase in fluorescence is completely eliminated (open triangles, CNQX + APV; $n = 8$).

Discussion

The calyx of Held–MNTB synapse provides a model system to analyze basic mechanisms of synaptic transmission. We have investigated the role of protons on synaptic transmission, acting through the activation of ASICs. We have demonstrated that MNTB neurons from mice respond to a drop in pH with an amiloride-sensitive transient inward current whose reversal potential was close to that of currents mediated by Na^+/Ca^{2+}, indicating that functional ASICs of the ENaC/degenerin family are expressed in these neurons. These ASIC-mediated currents were abolished by PcTx1, a toxin that specifically blocks homomeric ASIC-1a by increasing the pH sensitivity of steady-state desensitization and causing ASIC-1as to desensitize at pH 7.4 (Escoubas et al., 2000; Chen et al., 2006). The inhibition of I_{ASIC}s by PcTx1 in WT mice and the absence of currents in ASIC1a $^{-/-}$ mice identified homomeric ASIC-1as as the main isoform of ASICs in MNTB neurons. Furthermore, ASIC activation induced membrane depolarization and triggered action potentials in WT MNTB neurons, an effect that has been reported in cortical, hippocampal, retinal ganglion, and spinal cord neurons (Baron et al., 2002, 2008; Chu et al., 2004, Lilley et al., 2004; Wu et al., 2004). In contrast, no presynaptic I_{ASIC}s were observed in the nerve terminal during local acidification.

ASIC-1a has a low but significant permeability to Ca^{2+} that has been suggested to be physiologically relevant (Xiong et al., 2004, 2006; Yermolaieva et al., 2004; Ziemann et al., 2008). We have confirmed that ASIC-1a activation induces an increase in calcium influx into the postsynaptic cell, as indicated by the increase in fluorescence of the high-affinity Ca^{2+} indicator Fluo 8 during iontophoretic extracellular application of H^+ (Fig. 3*d*).

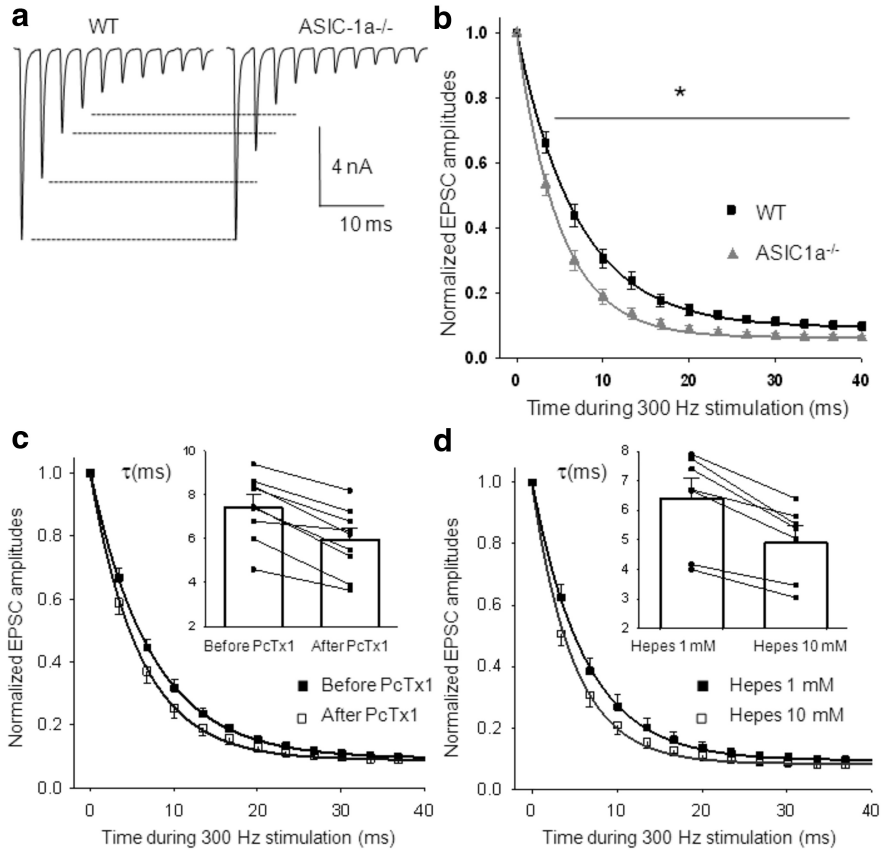

Figure 6. Enhanced STD at excitatory synaptic transmission in ASIC1a $^{-/-}$ mice compared with WT mice. ***a***, Representative recording of AP-evoked EPSCs in WT and ASIC1a $^{-/-}$ MNTB neurons during 300 Hz stimulation. ***b***, Time course of EPSC peak amplitudes (normalized to the first EPSC amplitude in the train) during 0.7 s stimulation at 300 Hz, fitted to a single exponential decay function, with a mean decay time constant $\tau = 7.0 \pm 0.5$ ms in WT mice ($n = 42$) and $\tau = 5.0 \pm 0.6$ ms in ASIC1a $^{-/-}$ mice ($n = 21$; $p = 0.01$, Student's *t* test). The EPSC amplitudes at the end of the stimuli reach a steady-state value of $9.3 \pm 0.2\%$ and $6.2 \pm 0.2\%$, respectively, of the first EPSC amplitude in the train, in WT and ASIC1a $^{-/-}$ mice ($p = 0.04$, Student's *t* test). $^*p < 0.05$, one-way repeated-measures ANOVA. ***c***, Effect of PcTx1 on STD in WT mice. Normalized EPSC amplitudes as a function of time recorded in WT MNTB neurons during 300 Hz stimulation in bicarbonate-based aCSF at pH 7.3 before (filled squares) and during (open squares) the application of PcTx1 in the external solution. Data fitted to a single exponential decay function show an enhanced STD when ASIC-1as are blocked (mean decay time constants: before application of PcTx1, $\tau = 7.3 \pm 0.6$ ms; after application of PcTx1, $\tau = 5.96 \pm 0.53$ ms; $n = 9$). Inset, Individual and mean τ values, $p = 4 \times 10^{-5}$, paired student's *t* test). Steady-state values of EPSC amplitudes at the end of the stimuli are also statistically different (before application of PcTx1, $9.4 \pm 0.7\%$ of the first EPSC amplitude in the train; after application of PcTx1, $8.8 \pm 0.8\%$ of the first EPSC amplitude in the train; $p = 0.002$, paired Student's *t* test). ***d***, Effect of pH buffering on STD in WT mice. Time course of normalized EPSC amplitudes during 300 Hz stimulation recorded sequentially in a 1 mM (filled squares) and 10 mM (open squares) HEPES/MES-based aCSF ($n = 8$), fitted by single exponential decay functions. When acidification is inhibited by a high-pH buffer capacity solution, STD is increased (mean decay time constants: HEPES 1 mM: $\tau = 6.4 \pm 0.7$ ms; HEPES 10 mM: $\tau = 4.9 \pm 0.6$ ms). Inset, Individual τ values and mean ($n = 8$, $p = 6 \times 10^{-4}$, paired Student's *t* test). Steady-state values of EPSC amplitudes at the end of the stimuli are $9.5 \pm 0.9\%$ vs $8.3 \pm 0.9\%$ of the first EPSC amplitude in the train, in HEPES 1 mM and HEPES 10 mM, respectively ($p = 0.005$, paired Student's *t* test).

Since ASICs are activated by extracellular protons, it is reasonable that they are involved in biological processes where extracellular acidosis occurs. The pH inside synaptic vesicles is acidic (pH < 6.0; Miesenböck et al., 1998), and protons are released from synaptic vesicles during synaptic transmission. These protons can lower the pH of the synaptic cleft (Krishtal et al., 1987; Trapp et al., 1996a,b) and affect pH-sensitive ion channel activity. Actually, we have identified ASIC-1a-dependent currents in MNTB neurons from WT mice during synaptic transmission whose amplitudes are small relative to glutamatergic AMPA-mediated EPSCs. These currents are blocked by amiloride and PcTx1 and are not observed in MNTB neurons from ASIC1a $^{-/-}$ mice. They are also inhibited when a high pH-buffering extracellular solution avoids acidification of the synaptic space or when ASICs are desensitized due to a sustained low pH of the extracellular solution (Fig. 4). Although small, these ASIC-1a-dependent signals could be relevant to synaptic transmission since they are able to generate APs in the absence of glutamatergic currents (Fig. 4*f*). However, it should be considered that our experimental conditions included AMPA, NMDA, GABA, and glycine receptor antagonists that can artificially increase the input resistance of the MNTB cells and, thus, may help the small ASIC EPSCs to evoke the postsynaptic spikes.

We also observed an increase in intracellular Ca^{2+} in MNTB neurons that can be assigned to a calcium influx through ASIC-1as activated by protons released from synaptic vesicles during physiological HFS of presynaptic terminals (Fig. 5). The Ca^{2+} signal throughout ASICs located at the postsynapsis is small compared with the signal generated by the activation of AMPA receptors but may serve a specific purpose, like modulating transmitter release, due to their localization and/or association with other signaling molecules linked to a specific pathway (Zha, 2013). At the postsynaptic sites, ASIC-1as have been linked to synaptic protein PICK1 (Hruska-Hageman et al., 2002; Jin et al., 2010). This interaction may be important for the localization and/or function of these channels in cell signaling. Given that, during synaptic transmission, the most likely source of protons is from presynaptic neurotransmitter-containing vesicles, detecting ASIC-dependent currents and Ca^{2+} influx reinforces the idea of protons acting as neurotransmitters in fast synapses. By contributing to neurotransmission, these results suggest that ASICs can modify membrane voltage and synaptic intracellular Ca^{2+}, modulating synaptic strength and plasticity.

The relevance of ASICs on transmitter release at the calyx of Held–MNTB synapse was investigated by comparing glutamatergic EPSCs in neurons from WT and ASIC1a $^{-/-}$ mice. EPSC amplitudes were not different between genotypes and were not affected by psalmotoxin. However, synaptic transmission during HFS, which induces maximal exocytosis of synaptic vesicle contents and extracellular reduction of pH, reveals a modulation of synaptic plasticity by ASIC activation. The lack of ASIC-1as or their pharmacological inhibition during presynaptic HFS results in a faster and stronger STD with lower steady-state values of EPSC amplitudes at the end of the stimuli. In WT mice, PcTx1 mimics the effect on STD that was observed on ASIC1a $^{-/-}$ mice (Fig. 6*c*), and the same happened when STD was measured in a high-pH buffer capacity aCSF that avoided acidification and the subsequent ASIC activation (Fig. 6*d*). Therefore, presynaptically re-

leased protons modulate presynaptic neurotransmitter release through the activation of the ASICs.

The quantal content of transmitter release during HFS is controlled by an intricate balance between Ca^{2+}-dependent depletion and the replenishment of synaptic vesicles. Previous studies (Cho et al., 2008) using microisland cultures of hippocampal neurons demonstrated increased probability of glutamate release in neurons from ASIC-1-lacking mice. Our group has also shown that pharmacological and genetic disruption of ASIC-1a activity resulted in an enhancement of transmitter release at the neuromuscular junction (Urbano et al., 2014). At the calyx of Held during HFS, no difference was observed in the initial EPSC, but a stronger reduction in amplitude was observed in the following EPSCs when ASICs were not active, indicating that, through an undisclosed pathway, ASIC activation increases probability of release or the size of the synaptic vesicle ready releasable pool. Future experiments aimed to interfere with a possible retrograde signal will provide important clues on the ASIC-dependent synaptic transmission neuromodulation system.

A pH modulation of the EPSCs by protons acting on the postsynaptic glutamate receptors cannot be ruled out. NMDA receptors are strongly inhibited by protons (Traynelis and Cull-Candy, 1991) and at physiologically relevant pH, protons inhibit glutamate AMPA-evoked currents and enhance the apparent rate and extent of AMPA receptor desensitization (Ihle and Patneau, 2000; Lei et al., 2001). Thus, during HFS, an increased rate of STD could result from an enhanced postsynaptic AMPA desensitization. However, in our hands, this mechanism does not seem to be physiologically relevant since changes in STD are observed in ASIC1a $^{-/-}$ mice and are mimicked by PcTx1 in WT mice.

Since ASICs were not observed at the presynpatic terminals, we assume that during HFS ASICs located at the MNTB neurons or astrocytes may trigger a retrograde signal toward the presynaptic terminal. Astrocytes surrounding the calyx of Held–MNTB synapse are part of the synaptic structure and extend their fine processes between the fingers of the calyx of Held and the principal neuron contacting both presynaptic and postsynaptic membranes (Renden et al., 2005; Reyes-Haro et al., 2010). Although the existence of ASICs has been shown in cultured astrocytes from rat cortical tissues (Huang et al., 2010), at present there is no information regarding the expression of ASICs in the calyx of Held astrocytes. The presynaptic modulation could also result from the action of pH changes on other ion channels or receptors like Ca^{2+} channels. In photoreceptor synapses, neurotransmission lowers pH sufficiently to inhibit presynaptic L-type Ca^{2+} channels, which mediate transmitter release (DeVries, 2001; Vessey et al., 2005). Also, proton-mediated blockage of Ca^{2+} channels during multivesicular release regulates short-term plasticity at auditory hair cell synapses (Cho and von Gersdorff, 2014). In contrast, P/Q-type channels, which mediate transmitter release at the developed calyx of Held, are poorly affected by pH changes (Shah et al., 2001; Cens et al., 2011). Furthermore, pH changes in the cleft are expected not to last long enough to modulate the calcium current generated by the next action potential during HFS.

What is the physiological role of proton–ASIC signaling in neurotransmission? Compared with AMPA-mediated glutamatergic currents, ASIC currents make a very small contribution to EPSCs induced by a single pulse. Proton signals may be particularly important during intense presynaptic stimulation where glutamatergic signals are subject to receptor desensitization. The combination of unusually fast deactivation with slow desensitization enables ASICs to follow trains of brief stimuli at high frequencies, suggesting that they may sustain postsynaptic responses when other receptors desensitize (MacLean and Jayaraman, 2016). A hypothesis to be tested at the calyx of Held from young animals, where postsynaptic glutamate receptors are highly desensitized by HFS. Furthermore, the Ca^{2+} signal detected through ASIC-1as may serve a specific purpose due to the localization and or association with other signaling molecules. These effects could explain the involvement of protons and the requirement of ASICs for long-term potentiation induced by HFS (Wemmie et al., 2002).

In summary, our results support the concept that protons coreleased with glutamate act as neurotransmitters during acidification of the synaptic cleft. Electrophysiological recordings and Ca^{2+} imaging studies demonstrate that ASICs are the main postsynaptic proton receptors in the MNTB. The distribution and pH sensitivity of ASICs put them in a perfect position to sense pH reduction at a pH of ~7. Activation of ASICs modulates transmitter release and synaptic plasticity (short-term plasticity). Short-term plasticity is important in processing information in neural networks (e.g., producing a reliable response to repetitive activity), and, thus, changes in short-term plasticity may affect cognitive function, which is not surprising after taking into account that ASIC1 are required for normal behavioral responses to stresses such as amygdala-dependent fear-related learning and memory (Wemmie et al., 2002, 2003, 2006). The consequences of ASIC1 disruption are complex and influence both presynaptic and postsynaptic mechanisms.

References

Baron A, Deval E, Salinas M, Lingueglia E, Voilley N, Lazdunski M (2002) Protein kinase C stimulates the acid-sensing ion channel ASIC2a via the PDZ domain-containing protein PICK1. J Biol Chem 277:50463–50468. CrossRef Medline

Baron A, Voilley N, Lazdunski M, Lingueglia E (2008) Acid sensing ion channels in dorsal spinal cord neurons. J Neurosci 28:1498–1508. CrossRef Medline

Cens T, Rousset M, Charnet P (2011) Two sets of amino acids of the domain I of Cav2.3 Ca^{2+} channels contribute to their high sensitivity to extracellular protons. Pflugers Arch 462:303–314. CrossRef Medline

Chen CC, England S, Akopian AN, Wood JN (1998) A sensory neuron-specific, proton-gated ion channel. Proc Natl Acad Sci U S A 95:10240–10245. CrossRef Medline

Chen X, Kalbacher H, Gründer S (2006) Interaction of acid-sensing ion channel (ASIC) 1 with the tarantula toxin psalmotoxin 1 is state dependent. J Gen Physiol 127:267–276. CrossRef Medline

Chesler M (2003) Regulation and modulation of pH in the brain. Physiol Rev 83:1183–1221. CrossRef Medline

Cho JH, Askwith CC (2008) Presynaptic release probability is increased in hippocampal neurons from ASIC1 knockout mice. J Neurophysiol 99:426–441. CrossRef Medline

Cho S, von Gersdorff H (2014) Proton-mediated block of Ca^{2+} channels during multivesicular release regulates short-term plasticity at an auditory hair cell synapse. J Neurosci 34:15877–15887. CrossRef Medline

Chu XP, Xiong ZG (2012) Physiological and pathological functions of acid-sensing ion channels in the central nervous system. Curr Drug Targets 13:263–271. CrossRef Medline

Chu XP, Wemmie JA, Wang WZ, Zhu XM, Saugstad JA, Price MP, Simon RP, Xiong ZG (2004) Subunit-dependent high-affinity zinc inhibition of acid-sensing ion channels. J Neurosci 24:8678–8689. CrossRef Medline

DeVries SH (2001) Exocytosed protons feedback to suppress the Ca^{2+} current in mammalian cone photoreceptors. Neuron 32:1107–1117. CrossRef Medline

Du J, Reznikov LR, Price MP, Zha XM, Lu Y, Moninger TO, Wemmie JA, Welsh MJ (2014) Protons and ASICs are a neurotransmitter/receptor pair that regulates synaptic plasticity in the lateral amygdala. Proc Natl Acad Sci U S A 111:8961–8966. CrossRef Medline

Escoubas P, De Weille JR, Lecoq A, Diochot S, Waldmann R, Champigny G, Moinier D, Ménez A, Lazdunski M (2000) Isolation of a tarantula toxin specific for a

class of proton-gated Na^+ channels. J Biol Chem 275:25116–25121. CrossRef Medline

Friese MA, Craner MJ, Etzensperger R, Vergo S, Wemmie JA, Welsh MJ, Vincent A, Fugger L (2007) Acid-sensing ion channel-1 contributes to axonal degeneration in autoimmune inflammation of the central nervous system. Nat Med 13:1483–1489. CrossRef Medline

Gründer S, Pusch M (2015) Biophysical properties of acid-sensing ion channels (ASICs). Neuropharmacology 94:9–18. CrossRef Medline

Hnasko TS, Edwards RH (2012) Neurotransmitter corelease: mechanism and physiological role. Annu Rev Physiol 74:225–243. CrossRef Medline

Hruska-Hageman AM, Wemmie JA, Price MP, Welsh MJ (2002) Interaction of the synaptic protein PICK1 (protein interacting with C kinase 1) with the non-voltage gated sodium channels BNC1 (brain Na^+ channel 1) and ASIC (acid-sensing ion channel). Biochem J 361:443–450. CrossRef Medline

Huang C, Hu ZL, Wu WN, Yu DF, Xiong QJ, Song JR, Shu Q, Fu H, Wang F, Chen JG (2010) Existence and distinction of acid-evoked currents in rat astrocytes. Glia 58:1415–1424. CrossRef Medline

Huang Y, Jiang N, Li J, Ji YH, Xiong ZG, Zha XM (2015) Two aspects of ASIC function: synaptic plasticity and neuronal injury. Neuropharmacology 94:42–48. CrossRef Medline

Ihle EC, Patneau DK (2000) Modulation of a-amino-3-hydroxy-5-methyl-4-isoxazolepropionic acid receptor desensitization by extracellular protons. Mol Pharmacol 58:1204–1212. CrossRef Medline

Jin W, Shen C, Jing L, Zha XM, Xia J (2010) PICK1 regulates the trafficking of ASIC1a and acidotoxicity in a BAR domain lipid binding-dependent manner. Mol Brain 3:39. CrossRef Medline

Kellenberger S, Schild L (2015) International Union of Basic and Clinical Pharmacology. XCI. Structure, function, and pharmacology of acid-sensing ion channels and the epithelial Na^+ channel. Pharmacol Rev 67:1–35. CrossRef Medline

Kreple CJ, Lu Y, Taugher RJ, Schwager-Gutman AL, Du J, Stump M, Wang Y, Ghobbeh A, Fan R, Cosme CV, Sowers LP, Welsh MJ, Radley JJ, LaLumiere RT, Wemmie JA (2014) Acid-sensing ion channels contribute to synaptic transmission and inhibit cocaine-evoked plasticity. Nat Neurosci 17:1083–1091. CrossRef Medline

Krishtal O (2003) The ASICs: signaling molecules? Modulators? Trends Neurosci 26:477–483. CrossRef Medline

Krishtal OA, Osipchuk YV, Shelest TN, Smirnoff SV (1987) Rapid extracellular pH transients related to synaptic transmission in rat hippocampal slices. Brain Res 436:352–356. CrossRef Medline

Lei S, Orser BA, Thatcher GR, Reynolds JN, MacDonald JF (2001) Positive allosteric modulators of AMPA receptors reduce proton-induced receptor desensitization in rat hippocampal neurons. J Neurophysiol 85:2030–2038. Medline

Li T, Yang Y, Canessa CM (2012) Impact of recovery from desensitization on acid-sensing ion channel-1a (ASIC1a) current and response to high frequency stimulation. J Biol Chem 287:40680–40689. CrossRef Medline

Lilley S, LeTissier P, Robbins J (2004) The discovery and characterization of a proton-gated sodium current in rat retinal ganglion cells. J Neurosci 24:1013–1022. CrossRef Medline

Lingueglia E, de Weille JR, Bassilana F, Heurteaux C, Sakai H, Waldmann R, Lazdunski M (1997) A modulatory subunit of acid sensing ion channels in brain and dorsal root ganglion cells. J Biol Chem 272:29778–29783. CrossRef Medline

MacLean DM, Jayaraman V (2016) Acid-sensing ion channels are tuned to follow high-frequency stimuli. J Physiol 594:2629–2645. CrossRef Medline

Miesenböck G, De Angelis DA, Rothman JE (1998) Visualizing secretion and synaptic transmission with pH-sensitive green fluorescent proteins. Nature 394:192–195. CrossRef Medline

Palmer MJ, Hull C, Vigh J, von Gersdorff H (2003) Synaptic cleft acidification and modulation of short-term depression by exocytosed protons in retinal bipolar cells. J Neurosci 23:11332–11341. Medline

Price MP, Gong H, Parsons MG, Kundert JR, Reznikov LR, Bernardinelli L, Chaloner K, Buchanan GF, Wemmie JA, Richerson GB, Cassell MD, Welsh MJ (2014) Localization and behaviors in null mice suggest that ASIC1 and ASIC2 modulate responses to aversive stimuli. Genes Brain Behav 13:179–194. CrossRef Medline

Renden R, Taschenberger H, Puente N, Rusakov DA, Duvoisin R, Wang LY, Lehre KP, von Gersdorff H (2005) Glutamate transporter studies reveal the pruning of metabotropic glutamate receptors and absence of AMPA receptor desensitization at mature calyx of Held synapses. J Neurosci 25:8482–8497. CrossRef Medline

Reyes-Haro D, Müller J, Boresch M, Pivneva T, Benedetti B, Scheller A, Nolte C, Kettenmann H (2010) Neuron–astrocyte interactions in the medial nucleus of the trapezoid body. J Gen Physiol 135:583–594. CrossRef Medline

Shah MJ, Meis S, Munsch T, Pape HC (2001) Modulation by extracellular pH of low- and high-voltage-activated calcium currents of rat thalamic relay neurons. J Neurophysiol 85:1051–1058. Medline

Trapp S, Lückermann M, Kaila K, Ballanyi K (1996a) Acidosis of hippocampal neurons mediated by a plasmalemmal Ca^{2+}/H^+ pump. Neuroreport 7:2000–2004. CrossRef Medline

Trapp S, Lückermann M, Brooks PA, Ballanyi K (1996b) Acidosis of rat dorsal vagal neurons in situ during spontaneous and evoked activity. J Physiol 496:695–710. CrossRef Medline

Traynelis SF, Cull-Candy SG (1991) Pharmacological properties and H^+ sensitivity of excitatory amino acid receptor channels in rat cerebellar granule neurones. J Physiol 433:727–763. CrossRef Medline

Urbano FJ, Lino NG, González-Inchauspe C, González LE, Colettis N, Vattino LG, Wunsch AM, Wemmie, JA and. Uchitel OD (2014) Acid-sensing ion channels 1a (ASIC1a) inhibit neuromuscular transmission in female mice. Am J Physiol Cell Physiol 306:396–406. CrossRef Medline

Vessey JP, Stratis AK, Daniels BA, Da Silva N, Jonz MG, Lalonde MR, Baldridge WH, Barnes S (2005) Proton-mediated feedback inhibition of presynaptic calcium channels at the cone photoreceptor synapse. J Neurosci 25:4108–4117. CrossRef Medline

Waldmann R, Lazdunski M (1998) H(+)-gated cation channels: neuronal acid sensors in the NaC/DEG family of ion channels. Curr Opin Neurobiol 8:418–424. CrossRef Medline

Waldmann R, Champigny G, Bassilana F, Heurteaux C, Lazdunski M (1997a) A proton-gated cation channel involved in acid-sensing. Nature 386:173–177. CrossRef Medline

Waldmann R, Bassilana F, de Weille J, Champigny G, Heurteaux C, Lazdunski M (1997b) Molecular cloning of a non-inactivating proton-gated Na^+ channel specific for sensory neurons. J Biol Chem 272:20975–20978. CrossRef Medline

Wemmie JA, Chen J, Askwith CC, Hruska-Hageman AM, Price MP, Nolan BC, Yoder PG, Lamani E, Hoshi T, Freeman JH Jr, Welsh MJ (2002) The acid activated ion channel ASIC contributes to synaptic plasticity, learning, and memory. Neuron 34:463–477. CrossRef Medline

Wemmie JA, Askwith CC, Lamani E, Cassell MD, Freeman JH Jr, Welsh MJ (2003) Acid-sensing ion channel 1 is localized in brain regions with high synaptic density and contributes to fear conditioning. J Neurosci 23:5496–5502. Medline

Wemmie JA, Price MP, Welsh MJ (2006) Acid-sensing ion channels: advances, questions and therapeutic opportunities. Trends Neurosci 29:578–586. CrossRef Medline

Wu LJ, Duan B, Mei YD, Gao J, Chen JG, Zhuo M, Xu L, Wu M, Xu TL (2004) Characterization of acid-sensing ion channels in dorsal horn neurons of rat spinal cord. J Biol Chem 279:43716–43724. CrossRef Medline

Xiong ZG, Zhu XM, Chu XP, Minami M, Hey J, Wei WL, MacDonald JF, Wemmie JA, Price MP, Welsh MJ, Simon RP (2004) Neuroprotection in ischemia: blocking calcium-permeable acid-sensing ion channels. Cell 118:687–698. CrossRef Medline

Xiong ZG, Chu XP, Simon RP (2006) Ca^{2+}-permeable acid-sensing ion channels and ischemic brain injury. J Membr Biol 209:59–68. CrossRef Medline

Yermolaieva O, Leonard AS, Schnizler MK, Abboud FM, Welsh MJ (2004) Extracellular acidosis increases neuronal cell calcium by activating acid sensing ion channel 1a. Proc Natl Acad Sci U S A 101:6752–6757. CrossRef Medline

Zha XM (2013) Acid-sensing ion channels: trafficking and synaptic function. Mol Brain 6:1. CrossRef Medline

Ziemann AE, Schnizler MK, Albert GW, Severson MA, Howard MA 3rd, Welsh MJ, Wemmie JA (2008) Seizure termination by acidosis depends on ASIC1a. Nat Neurosci 11:816–822. CrossRef Medline